



ZIF-67 with precursor concentration-dependence morphology for aerobic oxidation of toluene



Yepeng Xiao ^{a,b}, Bingcheng Song ^a, Yaju Chen ^a, Lihua Cheng ^{a,b,c}, Qinggang Ren ^{a,*}

^a College of Chemical Engineering, Guangdong University of Petrochemical Technology, Maoming, China

^b Guangdong Provincial Engineering Technology Research Center of Petrochemical Corrosion and Safety, Guangdong University of Petrochemical Technology, Maoming, China

^c Key Laboratory of Inferior Crude Oil Processing of Guangdong Provincial Higher Education Institutes, Maoming, China

ARTICLE INFO

Article history:

Received 1 August 2020

Revised 9 October 2020

Accepted 26 October 2020

Available online 27 October 2020

Keywords:

Toluene

Oxidation

ZIF-67

Morphological control

ABSTRACT

Designing high-efficiency catalyst for the oxidation of toluene (TOL) into value-added products like benzyl alcohol, benzaldehyde and benzoic acid is of great significance in chemical industry. Herein, four type of ZIF-67 with different morphology (ZIF-67-6, ZIF-67-12, ZIF-67-18, and ZIF-67-24) are prepared by tuning the concentration of precursor. About 90% of TOL conversion is obtained in the presence of ZIF-67-24 (0.1–0.2 μm , polyhedrons) by using O_2 (>99.9%, 1 atm) as oxidant at 40 °C after 4 h of reaction. Excellent performance of ZIF-67-24 could be attributed to two reasons: (I) The good crystallinity and smaller size with larger BET surface ($2037 \text{ m}^2 \text{ g}^{-1}$). (II) The electron deficient Co in ZIF-67-24 may be responded to the fast initiation of radical chain process of TOL oxidation. The research may provide a promising concept for oxidation of C-H under mild condition.

© 2020 Published by Elsevier B.V.

1. Introduction

Oxidation of toluene (TOL) is an important component of C-H activation. Its products (benzyl alcohol, benzaldehyde and benzoic acid) are in great demand in the chemical industry [1]. Although the oxidation of TOL has been industrialized as early as the mid-20th century, some problems exist in the catalytic system, such as using corrosive fatty acids as the solvent, using bromide as the initiator, and over-oxidation to deep oxidation products (such as CO_x) [2]. Hence, high-performance catalyst for oxidation of TOL is still in an urgent need.

Past decades have witnessed a rapid development in oxidative activation of C-H bonds, and the transition metals with half-full outer electron orbitals such as V, Cr, Mn, Fe, Co, Ni, Cu, Ce were one of the research hot spots. These transition metals and their oxide were selected as the active components to form metalloporphyrin [3], layered bimetallic hydroxide [4], heteropoly acid [5] and so on. Besides, supported catalysts ($\text{MnO}_x/\text{SBA}-15$ [6], $\text{MnO}_x/\text{ZSM-5}$ [7], $\text{FeO}_x/\text{SBA}-15$ [8], $\text{NiO}_x/\text{SBA}-15$ [9], $\text{CeO}_2/\text{Al}_2\text{O}_3$ [10], $\text{CuO}/\text{ZSM-5}$ [11], $\text{VOHPO}_4/\text{KIT}-6$ [12], CuCr_2O_4 [13], CoCuO_x [14], and V-Mo-Fe-O [15], etc) were widely reported, too. Due to the half-filled outer

electron orbitals, the superoxide intermediates accumulated during chain growth can be rapidly decomposed by such catalytic systems via the Haber-Weiss cycle [16,17]. However, the catalytic activity are greatly influenced by their morphology and dispersion [18–20]. Generally, well-dispersed active components with suitable morphology can efficiently stimulate the lattice oxygen of metallic oxide to participate in the reaction (mars-van krevelen redox reaction mechanism) [18,21]. Thus the formation of reactive oxygen species is accelerated, which can react with TOL by hydrogen extraction. As a result, the oxidation of TOL is facilitated. Recently, an important progress was made by Pappo's group [22]. Over 90% of conversion with 90% of selectivity to benzaldehyde was achieved in the oxidation of TOL using a cobalt acetate (catalyst)/ N-hydroxyphthalimide (NHPI, initiator)/ molecular oxygen (oxidant)/ 1,1,1,3,3-hexa-fluoropropan-2-ol (HFIP, solvent) system. However, the separation of homogeneous catalyst from reaction system is a obstacle for its further application in industry.

Metal-organic frameworks (MOFs) are inorganic-organic compounds with high surface areas and well-developed pores, which can afford them excellent performance in gas adsorption and separation [23,24], new energy production [25], catalysis [26,27] and so on. the properties of MOFs are significantly affected by a series of important factors, including the composition, morphology, defects and crystalline state [28]. However, one of the key doubts of

* Corresponding author.

E-mail address: 83842088@qq.com (Q. Ren).

utilizing MOFs in catalysis is their stability during the reaction process. Zeolitic imidazolate frameworks (ZIFs), a new class of MOFs that have exceptional chemical and thermal stability [29], are successfully applied in many reactions including oxidation of benzylic C-H bonds [30].

In this work, four type of ZIF-67 with different morphology are prepared by tuning the concentration of precursor. The catalytic activity of ZIF-67 (0.1–0.2 μm , polyhedrons) can be comparable with a homogeneous catalyst in the oxidation of TOL. The possible mechanism involved in the oxidation is also discussed.

2. Experimental

2.1. Catalysts preparation

The synthesis of ZIF-67 was similar to the previous literature with some modification [31]. Briefly, 3.75 mmol of $\text{Co}(\text{NO}_3)_2 \cdot 6\text{H}_2\text{O}$ and 7.5 mmol of 2-methylimidazole (Hmim) were dissolved in V mL ($V = 6, 12, 18, 24$) methanol to form clear solution, respectively. Then the two precursor solutions were mixed together under ultrasonic treatment for 5 min. After that, the mixture was maintained at room temperature for 24 h. The resulting samples were isolated via suction filtration, washed thoroughly with methanol, and finally dried in an oven at 70 °C overnight. The as-prepared products were marked as ZIF-67-V.

2.2. Catalysts characterization

Transmission electron microscopy (TEM) images were obtained by using a JEOL JEM-2010-TEM to determine the morphology of samples. X-ray diffraction (XRD) patterns of the catalysts were recorded with a Bruker D8 using $\text{Cu K}\alpha$ radiation. X-ray photoelectron spectroscopy (XPS) was performed by using an ULVAC PHI Quantera microscope. BET surface areas and pore structure were conducted with N_2 adsorption-desorption on a Micromeritics ASAP 2010 micropore analysis system. Electron paramagnetic resonance (EPR) spectra were collected by using a Bruker A300.

2.3. General procedure for toluene oxidation

The reaction was carried out in a head-space bottle (10 mL) with magnetic stirring at 25–40 °C under an O_2 (>99.9%, 1 atm) or air atmosphere. Firstly, 0.01 mmol catalysts were introduced into

the head-space bottle before screw the lid. After that, O_2 or air was pumped into the bottle for 5 min with two hollow needles. Then 0.50 mmol of toluene (TOL), 0.5 mL of 1,1,3,3-hexafluoropropan-2-ol (HFIP) with 0.025 mmol N-hydroxyphthalimide (NHPI) were injected into the bottle, following by 1 min of ultrasonic treatment. After the reaction was finished, the catalysts were separated by centrifugation. The reaction mixture was analyzed by an Agilent-7820A with a HP-5 capillary column and a flame ionization detector (FID), using ethylbenzene as an internal standard.

3. Results and discussion

3.1. Morphological and structural characterization

Fig. 1 shows that the morphology of ZIF-67 is depended by precursor concentration. A gradual change from flower-like nanostructure to polygon nanoparticles can be observed due to the dilution of $\text{Co}(\text{NO}_3)_2 \cdot 6\text{H}_2\text{O}$ and Hmim solutions by methanol simultaneously. As shown in **Fig. 1a**, the size of flower-like ZIF-67-6 is estimated about 1–2 μm , which is made up by smooth nanosheets (SEM images are presented in Fig. S1, Electronic supplementary information). Irregular blocks (ca. 1–2 μm) with nanosheets (100 nm in size) on the surface is presented from ZIF-67-12 (**Fig. 1b**). ZIF-67-18 is consisted by ~2 μm polyhedrons (**Fig. 1c**). Furthermore, **Fig. 1d** shows that the size of polyhedrons in ZIF-67-24 decreases to only 0.1–0.2 μm with reducing precursor concentration.

The XRD patterns of the as-prepared ZIF-67 with different precursor concentration are shown in **Fig. 2a**, matching well with previous report [32]. Higher crystallinity could be observed as a result of lower precursor concentration. As shown in **Fig. 2b**, photoelectron peaks of C, N, and Co elements are detected. The peak of O elements could be assigned to the absorbed water. The results of TEM, XRD and XPS confirm the successful preparation of the ZIF-67 samples.

As shown in **Fig. 3a** and b, according to IUPAC classification, typical IV type isotherm with a distinct hysteresis loop could be seen in ZIF-67-6 and ZIF-67-12, indicating the existence of mesopore (inserts in **Fig. 3a** and b, which may be resulted by the nanosheets structure). However, the curves in **Fig. 3c** and d are more closer to type I nitrogen isotherm, suggesting the presence of micropore structure (inserts in **Fig. 3c** and d). Moreover, other obtained data, including BET surface areas, total pore volumes and pore sizes, are summarized in **Table 1**.

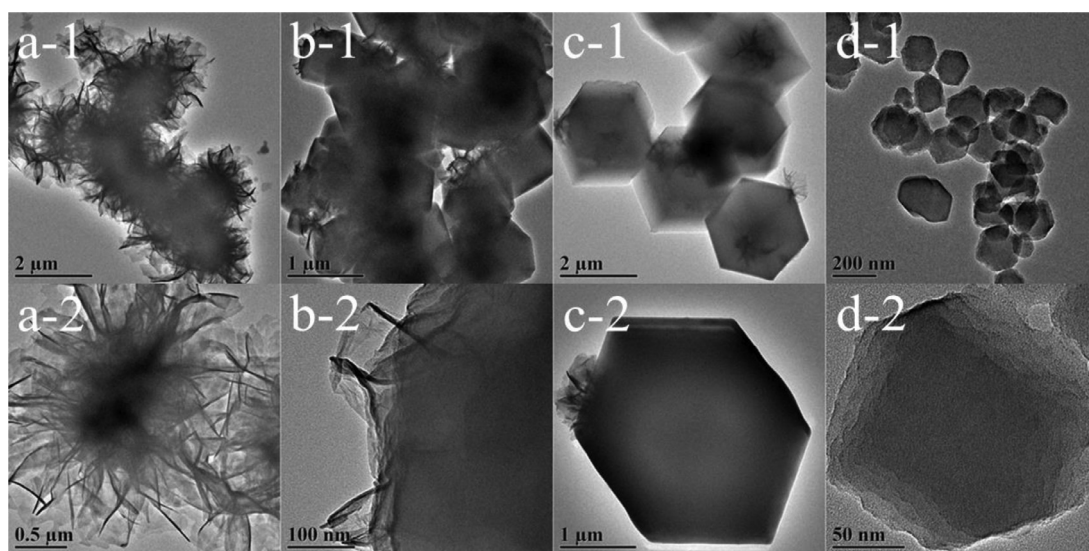


Fig. 1. TEM images of ZIF-67-6 (a), ZIF-67-12 (b), ZIF-67-18 (c) and ZIF-67-30 (d).

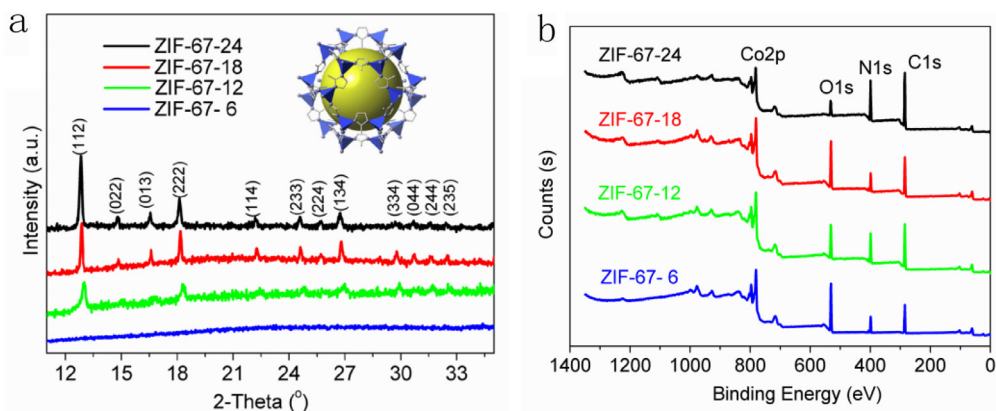


Fig. 2. XRD pattern (a) and XPS survy spectra (b) of ZIF-67-6, ZIF-67-12, ZIF-67-18, and ZIF-67-24.

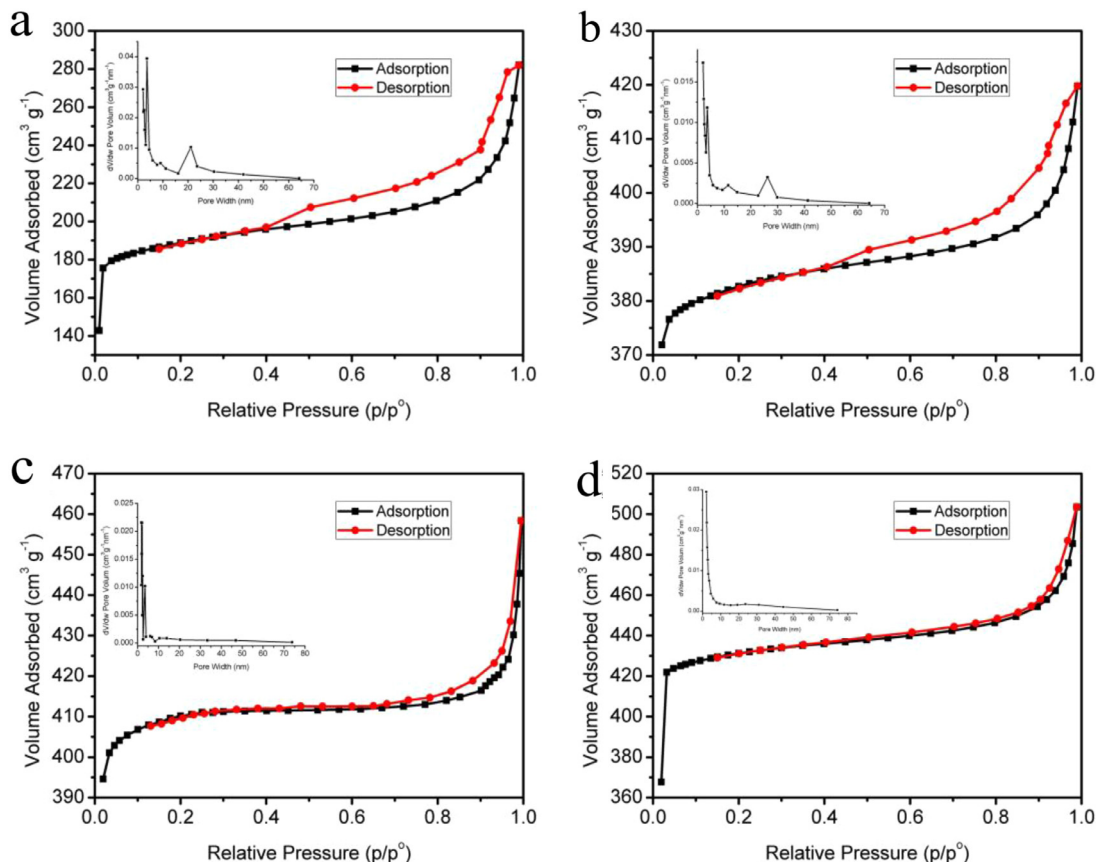


Fig. 3. N₂ adsorption-desorption isotherms of ZIF-67-6 (a), ZIF-67-12 (b), ZIF-67-18 (c), and ZIF-67-30 (d).

Table 1
BET surface areas, total pore volumes, and pore sizes for the synthesized samples.

Sample	BET surface area (m ² g ⁻¹)	Total pore volume (cm ³ g ⁻¹)	Average pore diameter (nm)
ZIF-67-6	800	0.436	2.18
ZIF-67-12	1722	0.649	1.51
ZIF-67-18	1719	0.709	1.65
ZIF-67-24	2037	0.779	1.53

3.2. Catalytic performance

The as-prepared ZIF-67 was employed as catalysts for the aerobic oxidation of TOL. The influence of various technological conditions on TOL catalytic oxidation reaction was summarizes in Fig. S2 (Electronic supplementary information). As shown in Table 2,

No apparent oxidative products is observed in a blank experiment, or in the presence of Co(NO₃)₂·6H₂O (Co(NO₃)₂·6H₂O could not be dissolved in HFIP) or Hmin, respectively. However, with ZIF-67-24 as catalyst, high-performance in catalytic efficiency is observed. 87.9% and 63.1% of TOL conversion are detected by using O₂ or air as oxidant, respectively (entry 4 and 5), which can be compara-

Table 2
Aerobic oxidation of TOL catalyzed by various catalysts^[a].

Entry	Catalysts	Conv. (%)	Select. (%)	Benzyl alcohol	Benzaldehyde	Benzyl acid
1	Blank	trace	–	–	–	–
2	Co(NO ₃) ₂ ·6H ₂ O	trace	–	–	–	–
3	Hmim	trace	–	–	–	–
4	ZIF-67-24	87.9	7.8	66.9	25.3	–
5 ^[b]	ZIF-67-24	63.1	20.4	70.7	8.9	–
6 ^[c]	ZIF-67-24	72.4	11.3	68.7	20.0	–
7 ^[d]	ZIF-67-24	54.1	18.1	64.2	17.7	–
8 ^[e]	Co(II)TPP	trace	–	–	–	–
9 ^[f]	Co(OAc) ₂ ·4H ₂ O	91	9	90	1	–
10 ^[g]	CoO _x /SiO ₂	91.2	8.4	68.8	20.3	–

^[a] Reaction conditions: TOL (0.5 mmol), NHPI (0.025 mmol), catalysts (0.01 mmol), O₂ (>99.9%, 1 atm), HFIP (0.5 mL), 40 °C, 4 h.

^[b] Use air as oxidant.

^[c] Reuse the catalysts from entry 4.

^[d] Reuse the catalysts from entry 5.

^[e] Use Co(II) meso-Tetraphenylporphine as catalyst.

^[f] Reference [21].

^[g] Reference [2].

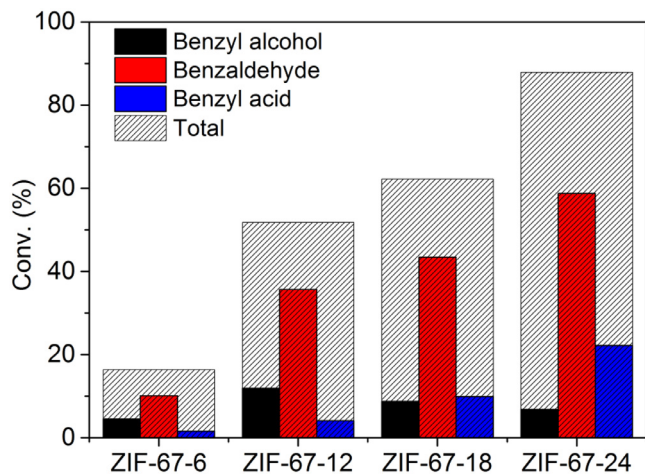


Fig. 4. Conversion efficiency of TOL oxidation catalyzed by ZIF-67-6, ZIF-67-12, ZIF-67-18, and ZIF-67-24. Reaction conditions: TOL (0.5 mmol), NHPI (0.025 mmol), catalysts (0.01 mmol), O₂ (> 99.9%, 1 atm), HFIP (0.5 mL), 40 °C, 4 h.

ble with a homogeneous catalyst (Co(OAc)₂·4H₂O, entry 8) [22] or a heterogeneous catalyst (CoO_x/SiO₂, entry 9) [2] in similar conditions. Unfortunately, the catalytic stability of ZIF-67-24 is dissatisfaction, nearly 40% of loss in conversion efficiency is observed after three consecutive runs. The poor stability may be caused by the exposition to benzoic acid, which could destroy the coordination structure of ZIF-67. This phenomenon is also found in other acid (such as acetic acid).

Generally, the catalytic behavior is greatly influenced by the morphology of catalyst. Hence, It is necessary to investigate the morphology of ZIF-67 with more effective for this oxidation process. As shown in Fig. 4, the conversions of TOL catalyzed by ZIF-67-6, ZIF-67-12, ZIF-67-18 and ZIF-67-24 are 16.4%, 51.8%, 62.2% and 87.9% after 4 h of reaction, respectively. Higher catalytic activity of ZIF-67-24 is obtained compared to that of ZIF-67-6, ZIF-67-12, and ZIF-67-18, implying that this oxidation process is facili-

tated by good crystallinity and smaller size with higher BET surface (2037 m² g⁻¹).

3.3. Study of probable mechanism

According to the earlier literature, the oxidation of TOL is involved in a free radical reaction, and the central atom Co(II) in ZIF-67 is proposed as the catalytic site. Fig. 5a shows the typical characteristic peaks of PINO (a free radical generated from NHPI) [33]. It is clear that the signal intensities have a good agreement with the catalytic performance. Fig. 5b shows the XPS spectra of Co 2p for ZIF-67-6, ZIF-67-12, ZIF-67-18 and ZIF-67-24. Comparing to the binding energy of Co 2p in ZIF-67-6, positive shifts in varying degrees are observed in ZIF-67-12 ($\Delta E = 0.2$ eV), ZIF-67-18 ($\Delta E = 0.4$ eV) and ZIF-67-24 ($\Delta E = 0.4$ eV), respectively. This phenomenon may be a result that less Co exist in the outer surface of ZIF-67-18 and ZIF-67-24, so their crystal structure is more complete (see Fig. 2a). As a result, the electron of Co may be disperse by its connected ligand. This electron deficient Co in ZIF-67-18 and ZIF-67-24 may have d-orbital vacancies, which will increase the donation to O₂ bonding orbital of the adsorbed O₂ formed during oxidation of TOL. Consequently, the bond between Co and O₂ is reinforced, which will do good to the formation of Co(III) complexes. As a result, the generation of PINO radical is facilitated by the reaction between Co(III) complexes and NHPI, which will speed up the initiation of radical chain process of TOL oxidation.

Based on the experimental results and the most accepted mechanism for the aerobic autoxidation reaction of methylarene by the NHPI/Co(OAc)₂ system proposed by Pappo's group [22], we conclude a possible reaction mechanism for catalytic oxidation of TOL over ZIF-67 (Fig. 6). This free radical reaction begins with the oxidation of Co(II) by molecular oxygen to afford Co(III) complexes (Step 1), which further react with NHPI to generate PINO radical (Step 2), so that the radical chain process is initiated. After that, benzyl radical is generated from hydrogen abstraction by the PINO radical (Step 3), readily reacts with molecular oxygen to eventually form benzyl peroxy radical (Step 4). In the step of chain termination (Step 5), benzyl alcohol and benzaldehyde, which could be

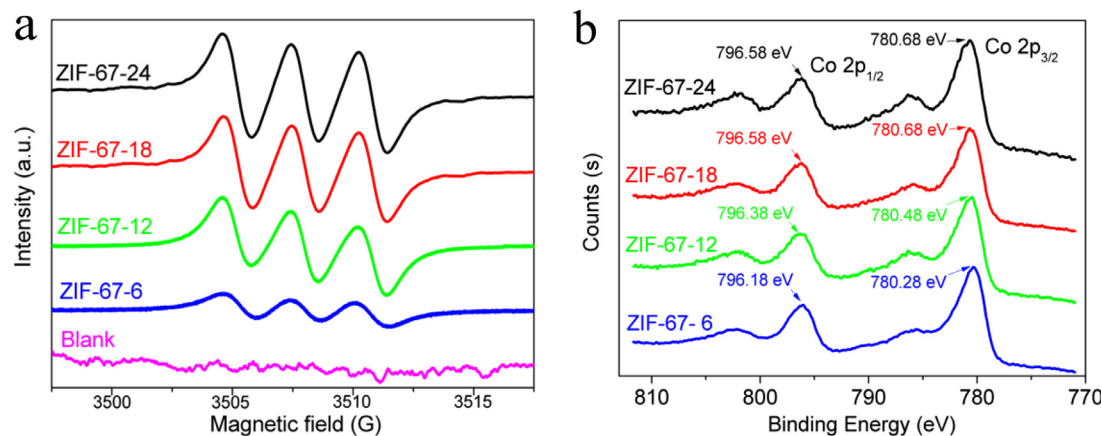


Fig. 5. ESR signals of the PINO (a), and XPS spectra of Co 2p (b) for ZIF-67-6, ZIF-67-12, ZIF-67-18, and ZIF-67-24. Reaction condition: 0.5 mmol of TOL, 0.025 mmol of NHPI, 0.01 mmol of catalysts, 1 atm of O₂, 0.5 mL of HFIP, 40 °C, 1 h.

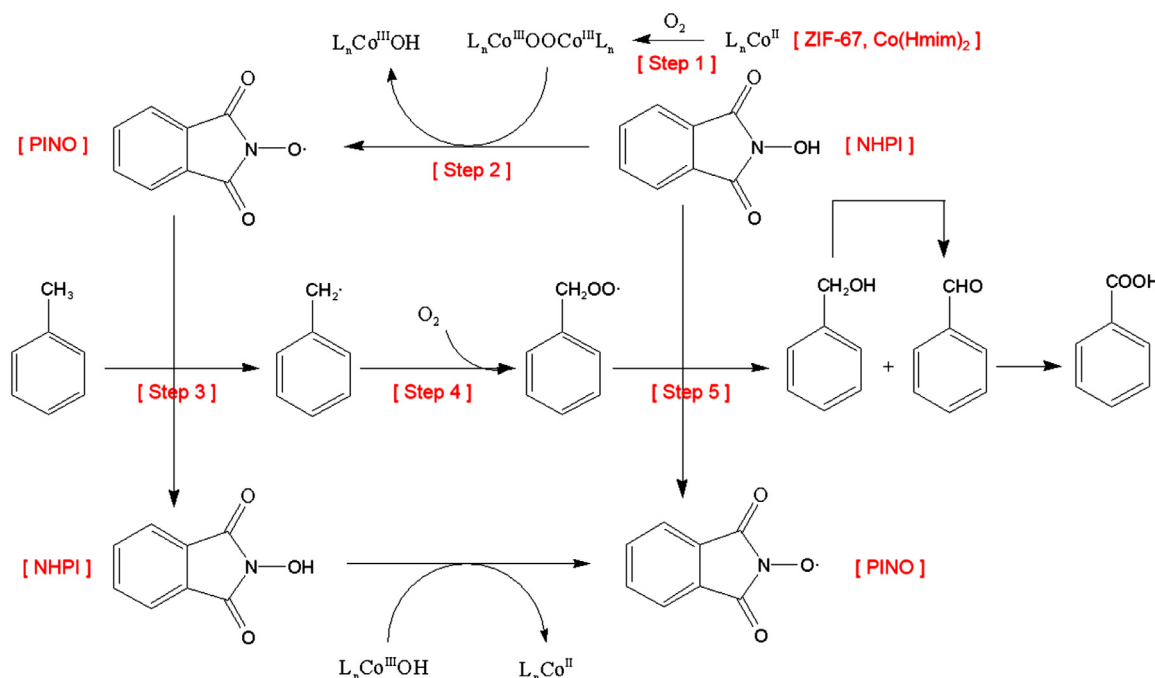


Fig. 6. The proposed mechanism for the aerobic catalyzed NHPI/ZIF-67 system of TOL.

further oxidized to benzyl acid, are formed by the mutual destruction of two benzyl peroxy radical.

4. Conclusion

In summary, by adjusting the concentration of precursor, a series of ZIF-67 (ZIF-67-6, ZIF-67-12, ZIF-67-18, and ZIF-67-24) with different morphology are prepared for TOL oxidation. Nearly 90% conversion of TOL is obtained in the presence of ZIF-67-24 by using O₂ (>99.9%, 1 atm) as oxidant at 40 °C after 4 h of reaction. Excellent performance of ZIF-67-24 could be attributed to the good crystallinity and smaller size with higher BET surface (2037 m² g⁻¹), and more importantly, the initiation of radical chain process of TOL oxidation may be accelerated by the electron deficient Co in ZIF-67-24. The research may propose a promising concept for oxidation of C-H under ambient condition.

Declaration of Competing Interest

None.

Acknowledgements

This work was financially supported by the Scientific Research Foundation for Advanced Talents of [Guangdong University of Petrochemical Technology](#) [No. 2018rc52], Special Fund for Science and Technology Innovation Strategy of Guangdong Province [No. 2018S00146], [Natural Science Foundation of Guangdong Province](#) [No. 2018A030307004] and Maoming Public Service Platform for Transformation Upgrading and Technological Innovation of Petrochemical Industry [No. 2016B020211001].

Supplementary materials

Supplementary material associated with this article can be found, in the online version, at [doi:10.1016/j.jorgchem.2020.121597](https://doi.org/10.1016/j.jorgchem.2020.121597).

References

- [1] C. Deng, M. Xu, Z. Dong, L. Li, J. Yang, X. Guo, L. Peng, N. Xue, Y. Zhu, W. Ding, Exclusively catalytic oxidation of toluene to benzaldehyde in an O/W emulsion stabilized by hexadecylphosphate acid terminated mixed-oxide nanoparticles, *Chinese J. Catal.* 41 (2020) 341–349.
- [2] G. Shi, S. Xu, Y. Bao, J. Xu, Y. Liang, Selective aerobic oxidation of toluene to benzaldehyde on immobilized CoO_x on SiO_2 catalyst in the presence of N-hydroxyphthalimide and hexafluoropropan-2-ol, *Catal. Commun.* 123 (2019) 73–78.
- [3] X.-L. Yang, M.-H. Xie, C. Zou, Y. He, B. Chen, M. O’Keeffe, C.-D. Wu, Porous metalloporphyrinic frameworks constructed from metal 5,10,15,20-te-trakis(3,5-biscarboxyphenyl)porphyrin for highly efficient and selective catalytic oxidation of alkylbenzenes, *J. Am. Chem. Soc.* 134 (2012) 10638–10645.
- [4] X. Wang, G. Wu, F. Wang, H. Liu, T. Jin, Solvent-free selective oxidation of toluene with O_2 catalysed by anion modified mesoporous mixed oxides with high thermal stability, *Catal. Commun.* 98 (2017) 107–111.
- [5] B. Ma, Z. Zhang, W. Song, X. Xue, Y. Yu, Z. Zhao, Y. Ding, Solvent-free selective oxidation of C-H bonds of toluene and substituted toluene to aldehydes by vanadium-substituted polyoxometalate catalyst, *J. Mol. Catal. A Chem.* 368 (2013) 152–158.
- [6] W. Zhong, S.R. Kirk, D. Yin, Y. Li, R. Zou, L. Mao, G. Zou, Solvent-free selective oxidation of toluene by oxygen over $\text{MnO}_x/\text{SBA}-15$ catalysts: relationship between catalytic behavior and surface structure, *Chem. Eng. J.* 280 (2015) 737–747.
- [7] Y. Meng, H.C. Genuino, C.-H. Kuo, H. Huang, S.-Y. Chen, L. Zhang, A. Rossi, S.L. Suib, One-step hydrothermal synthesis of manganese-containing MFI-type zeolite, Mn-ZSM-5, characterization, and catalytic oxidation of hydrocarbons, *J. Am. Chem. Soc.* 135 (2013) 8594–8605.
- [8] M. Lu, R. Huang, J. Wu, M. Fu, L. Chen, D. Ye, On the performance and mechanisms of toluene removal by $\text{FeO}_x/\text{SBA}-15$ -assisted non-thermal plasma at atmospheric pressure and room temperature, *Catal. Today* 242 (2015) 274–286.
- [9] W. Xu, X. Xu, J. Wu, M. Fu, L. Chen, N. Wang, H. Xiao, X. Chen, D. Ye, Removal of toluene in adsorption-discharge plasma systems over a nickel modified SBA-15 catalyst, *Rsc Adv.* 6 (2016) 104104–104111.
- [10] S.M. Saqer, D.I. Kondarides, X.E. Verykios, Catalytic oxidation of toluene over binary mixtures of copper, manganese and cerium oxides supported on gamma-Al₂O₃, *Appl. Catal., B* 103 (2011) 275–286.
- [11] N. Viswanadham, S.K. Saxena, A.H. Al-Muhtaseb, Cu functionalized nano crystalline ZSM-5 as efficient catalyst for selective oxidation of toluene, *Mater. Today Chem.* 3 (2017) 37–48.
- [12] M. Rezaei, A. Najafi Chermahini, H.A. Dabbagh, Selective oxidation of toluene to benzaldehyde by H_2O_2 with mesoporous silica KIT-6 supported VOHPO₄•5H₂O catalyst, *J. Environ. Chem. Eng.* 5 (2017) 3529–3539.
- [13] S.S. Acharyya, S. Ghosh, R. Tiwari, B. Sarkar, R.K. Singha, C. Pendem, T. Sasaki, R. Bal, Preparation of the CuCr₂O₄ spinel nanoparticles catalyst for selective oxidation of toluene to benzaldehyde, *Green Chem.* 16 (2014) 2500–2508.
- [14] R. Xie, G. Fan, L. Yang, F. Li, Hierarchical flower-like Co-Cu mixed metal oxide microspheres as highly efficient catalysts for selective oxidation of ethylbenzene, *Chem. Eng. J.* 288 (2016) 169–178.
- [15] H. Xia, Z. Liu, Y. Xu, J. Zuo, Z. Qin, Highly efficient V-Mo-Fe-O catalysts for selective oxidation of toluene to benzaldehyde, *Catal. Commun.* 86 (2016) 72–76.
- [16] B.P.C. Hereijgers, B.M. Weckhuysen, Aerobic oxidation of cyclohexane by gold-based catalysts: new mechanistic insight by thorough product analysis, *J. Catal.* 270 (2010) 16–25.
- [17] Y. Xiao, J. Liu, H. Wang, C. Yang, H. Cheng, Y. Deng, Y. Fang, Photothermal oxidation of cyclohexane by graphene oxide-based composites with high selectivity to KA oil, *Mol. Catal.* 493 (2020) 1–8.
- [18] R. Peng, S. Li, X. Sun, Q. Ren, L. Chen, M. Fu, J. Wu, D. Ye, Size effect of Pt nanoparticles on the catalytic oxidation of toluene over Pt/CeO₂ catalysts, *Appl. Catal., B* 220 (2018) 462–470.
- [19] Y. Xiao, J. Liu, K. Xie, W. Wang, Y. Fang, Aerobic oxidation of cyclohexane catalyzed by graphene oxide: effects of surface structure and functionalization, *Mol. Catal.* 431 (2017) 1–8.
- [20] Y. Xiao, J. Liu, Y. Lin, W. Lin, Y. Fang, Novel graphene oxide-silver nanorod composites with enhanced photocatalytic performance under visible light irradiation, *J. Alloys Compd.* 698 (2017) 170–177.
- [21] R.K. Grasselli, Fundamental principles of selective heterogeneous oxidation catalysis, *Top. Catal.* 21 (2002) 79–88.
- [22] E. Gaster, S. Kozuch, D. Pappo, Selective aerobic oxidation of methylarenes to benzaldehydes catalyzed by N-hydroxyphthalimide and cobalt(II) acetate in hexafluoropropan-2-ol, *Angew. Chem. Int. Ed.* 56 (2017) 5912–5915.
- [23] Z. Yan, Y. Gong, B. Chen, X. Wu, Q. Liu, L. Cui, S. Xiong, S. Peng, Methyl functionalized Zr-Fum MOF with enhanced Xenon adsorption and separation, *Sep. Purif. Technol.* 239 (2020).
- [24] T. Rodenas, I. Luz, G. Prieto, B. Seoane, H. Miro, A. Corma, F. Kapteijn, F.X. Llabres i Xamena, J. Gascon, Metal-organic framework nanosheets in polymer composite materials for gas separation, *Nature Mater.* 14 (2015) 48–55.
- [25] D. Sheberla, J.C. Bachman, J.S. Elias, C.-J. Sun, Y. Shao-Horn, M. Dinca, Conductive MOF electrodes for stable supercapacitors with high areal capacitance, *Nature Mater.* 16 (2017) 220–224.
- [26] Y. Luo, Y. Zheng, J. Zuo, X. Feng, X. Wang, T. Zhang, K. Zhang, L. Jiang, Insights into the high performance of Mn-Co oxides derived from metal organic frameworks for total toluene oxidation, *J. Hazard. Mater.* 349 (2018) 119–127.
- [27] Z. Sun, G. Li, Y. Zhang, H.-o. Liu, X. Gao, Ag-Cu-BTC prepared by postsynthetic exchange as effective catalyst for selective oxidation of toluene to benzaldehyde, *Catal. Commun.* 59 (2015) 92–96.
- [28] J. Duan, Y. Li, Y. Pan, N. Behera, W. Jin, Metal-organic framework nanosheets: an emerging family of multifunctional 2D materials, *Coord. Chem. Rev.* 395 (2019) 25–45.
- [29] K. Zhou, B. Mousavi, Z. Luo, S. Phatanasri, S. Chaemchuen, F. Verpoort, Characterization and properties of Zn/Co zeolitic imidazolate frameworks vs. ZIF-8 and ZIF-67, *J. Mater. Chem. A* 5 (2017) 952–957.
- [30] C. Guo, Y. Zhang, X. Nan, C. Feng, Y. Guo, J. Wang, Efficient selective catalytic oxidation of benzylic C-H bonds by ZIF-67 under eco-friendly conditions, *Mol. Catal.* 440 (2017) 168–174.
- [31] H. Chen, K. Shen, Q. Mao, J. Chen, Y. Li, Nanoreactor of MOF-derived yolk-shell Co@C-N: precisely controllable structure and enhanced catalytic activity, *ACS Catal.* 8 (2018) 1417–1426.
- [32] G. Wei, Z. Zhou, X. Zhao, W. Zhang, C. An, Ultrathin metal-organic framework nanosheet-derived ultrathin Co₃O₄ nanomeshes with robust oxygen-evolving performance and asymmetric supercapacitors, *ACS Appl. Mater. Inter.* 10 (2018) 23721–23730.
- [33] L. Wang, Y. Zhang, R. Du, H. Yuan, Y. Wang, J. Yao, H. Li, Selective one-step aerobic oxidation of cyclohexane to e-caprolactone mediated by N-hydroxyphthalimide (NHPI), *ChemCatChem* 11 (2019) 2260–2264.